Observational cosmology journal club: April 25, 2011

1. Supernova constraints and systematic uncertainties from the first three years of the supernova legacy survey, A.Conley et al. arXiv:1104.1443
2. SNLS3: Constraints on dark energy combining the supernova legacy survey three year data with other probes, M.Sullivan et al. arXiv:1104.1444
3. The Kepler cluster study: stellar rotation in NGC6811, S.Meibom et al. arXiv:1104.2912
4. Warm Saturns: on the nature of rings around extrasolar planets that reside inside the ice line, H.E.Schlighting & P.Chang. arXiv:1104.3863

A.Conley et al. : SNLS3

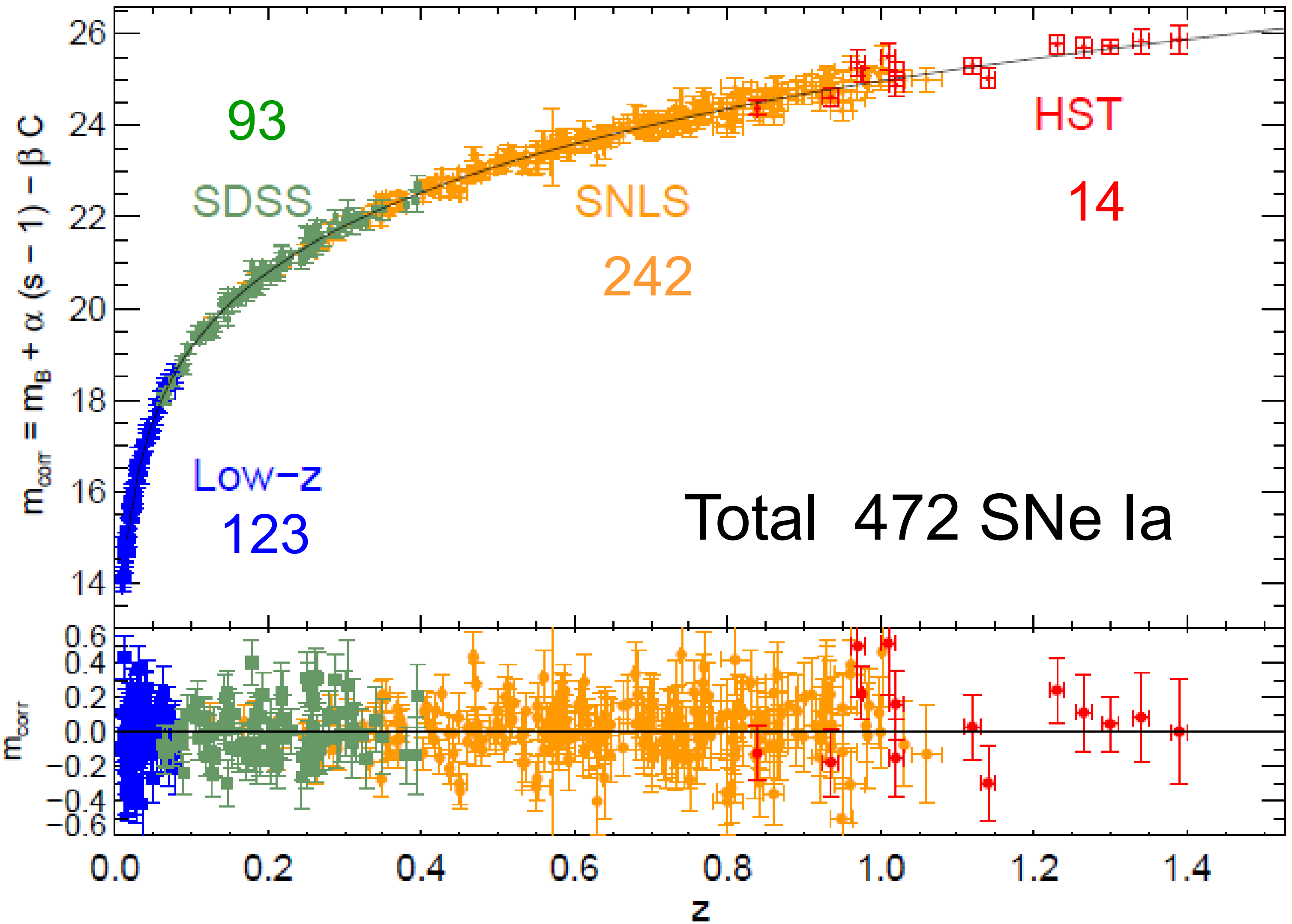

A.Conley et al. : SNLS3

$$
\begin{aligned}
m_B^{\mathrm{model}} = {} & 5\log_{10} D_L(z_{hel}, z_{CMB}, w, \Omega_m, \Omega_{DE}, \Omega_K) \\
& - \alpha(s-1) + \beta C \\
& + M_B + 5\log_{10}(c/H_0) + 25
\end{aligned}
$$

- s: stretch factor
- C: color measure
- 光度と、sおよびCとの経験的相関係数がαとβ

A.Conley et al. : SNLS3

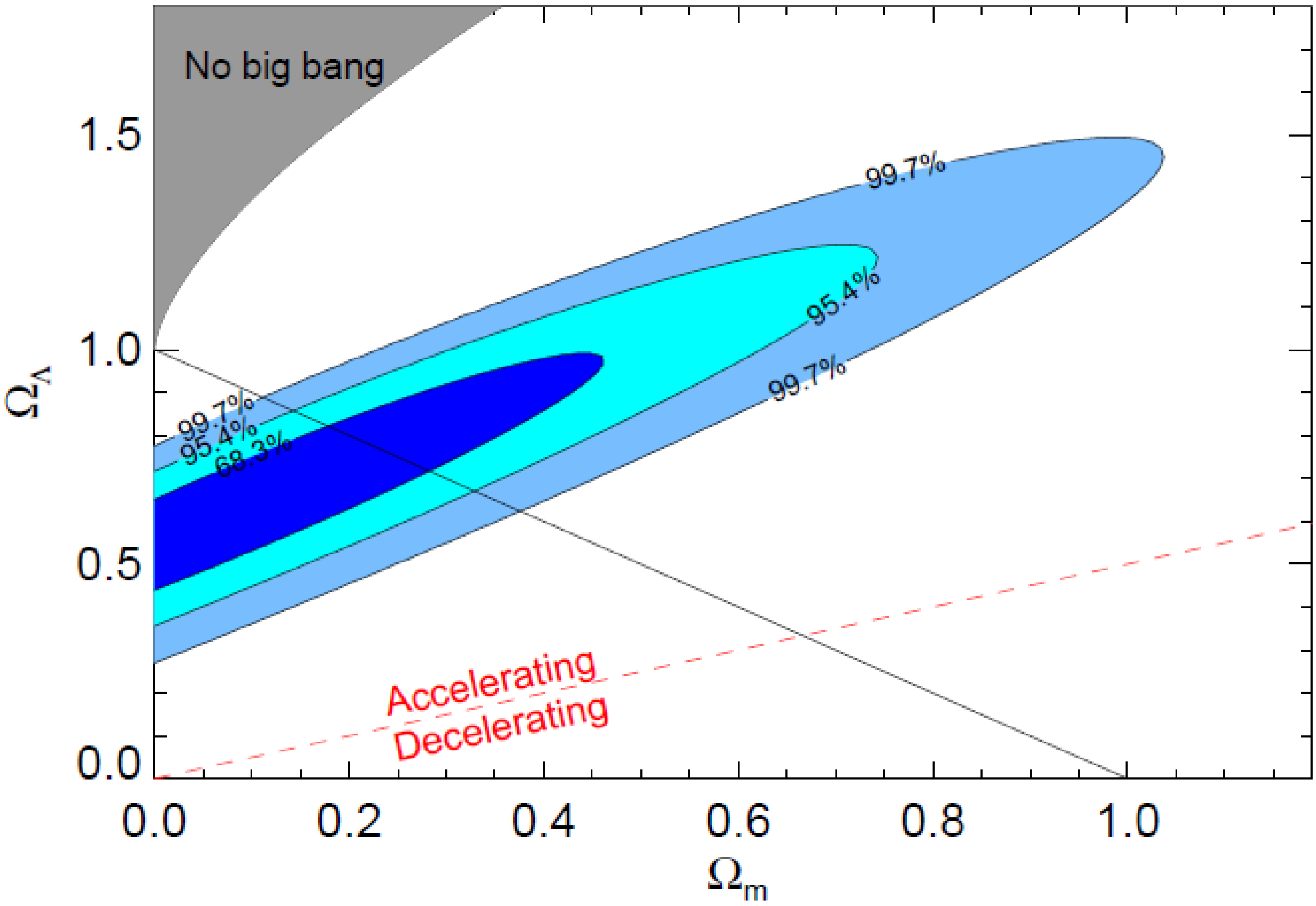

A.Conley et al. : SNLS3

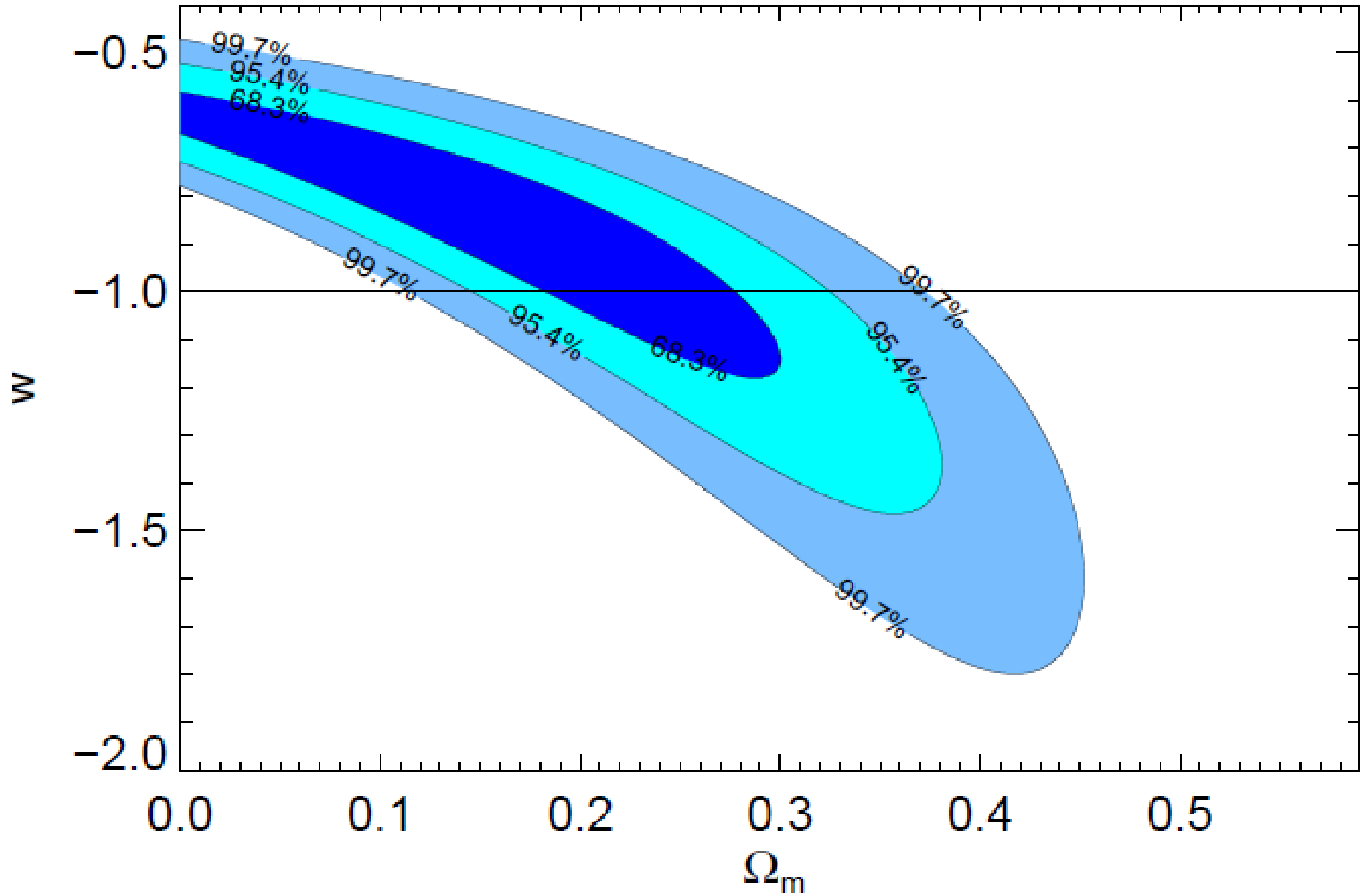

A.Conley et al. : SNLS3

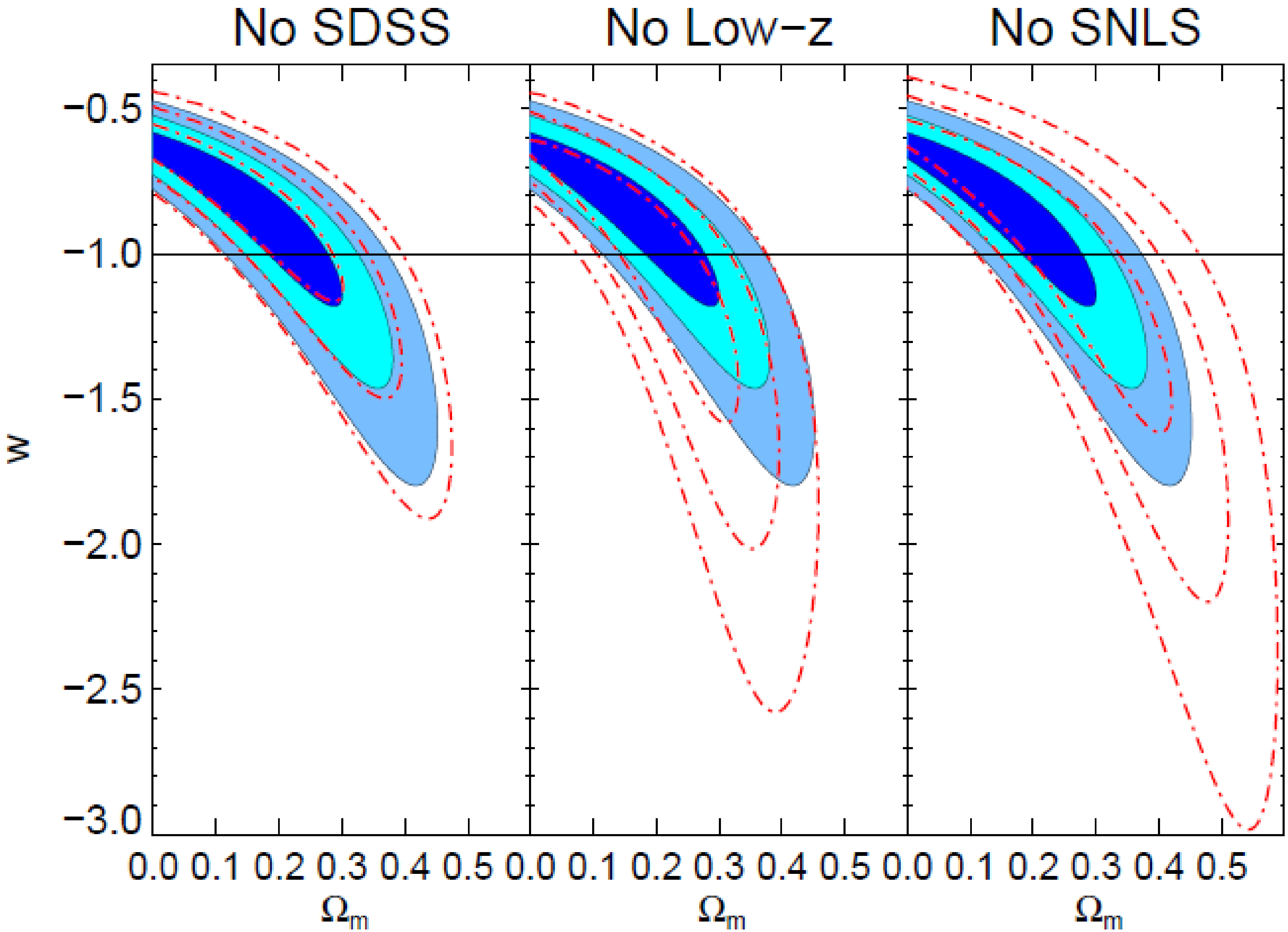

M.Sullivan et al. : SNLS3+

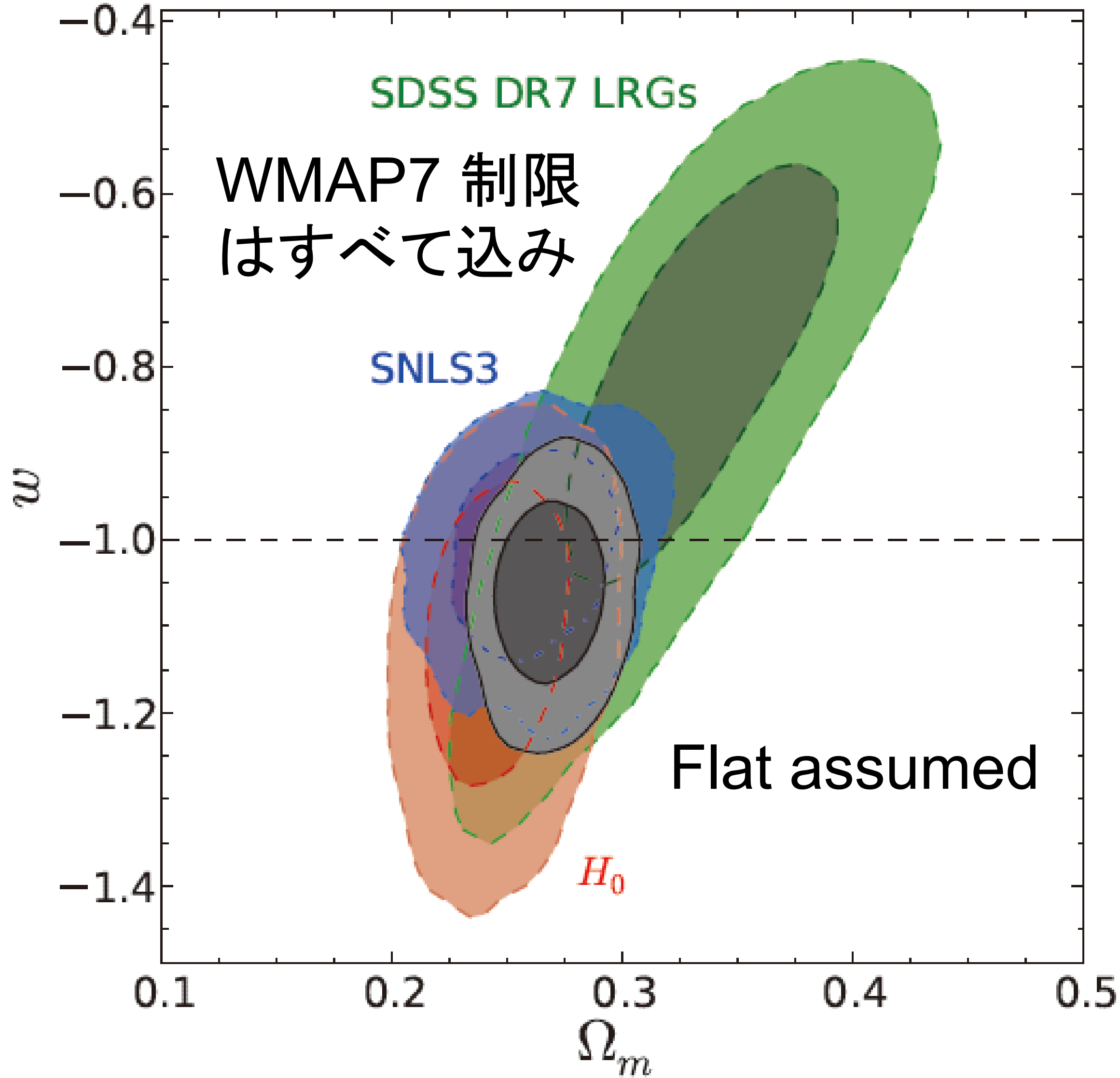

M.Sullivan et al. : SNLS3+

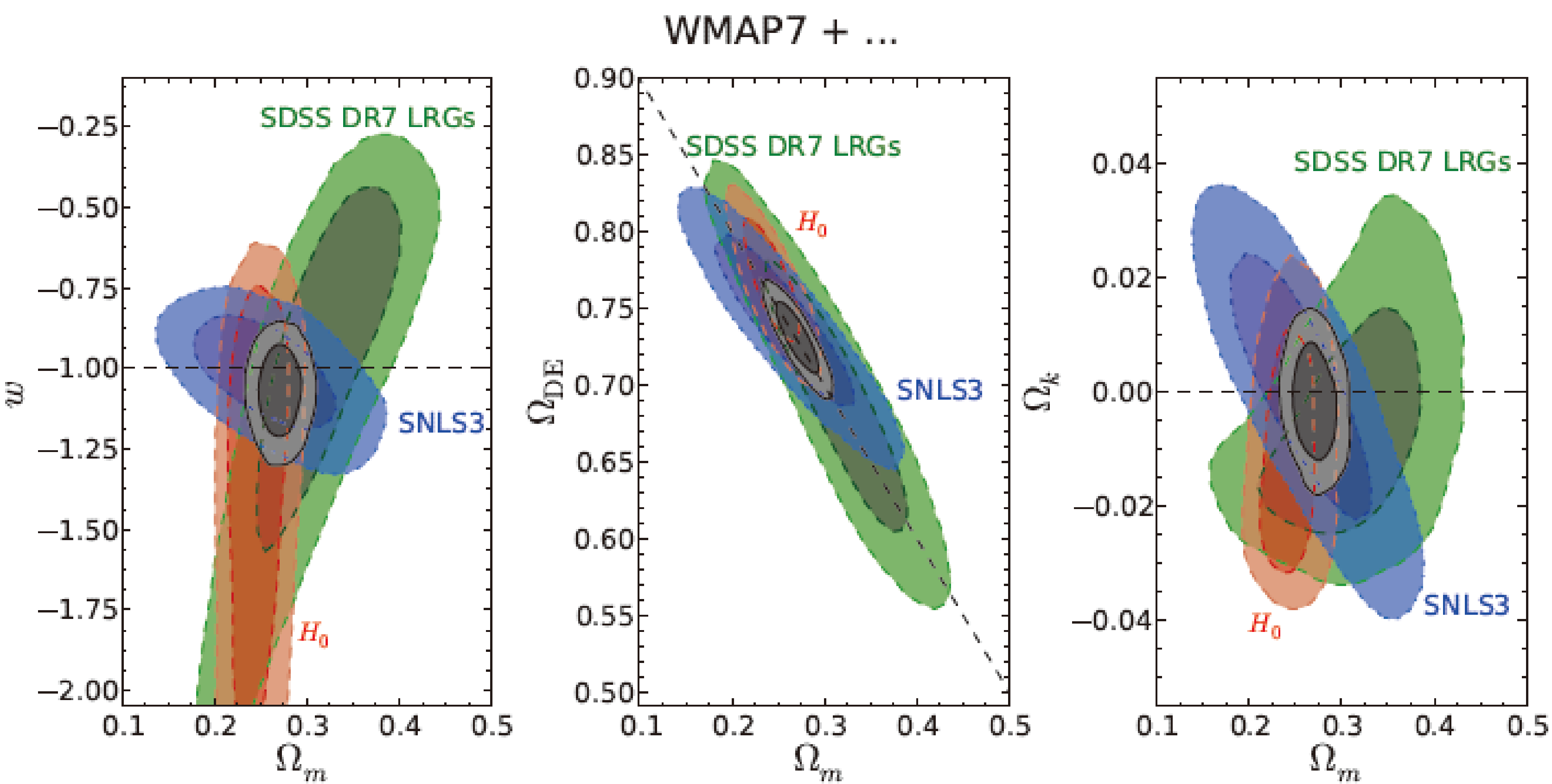

Flat universe is not assumed

M.Sullivan et al. : SNLS3+

Table 4. Cosmological results[a] obtained using the CosmoMC fitter with a constant dark energy equation of state

Parameter	WMAP7+SNLS3	WMAP7+DR7	WMAP7+$H0$[b]	WMAP7+DR7 +H_0	WMAP7+DR7 +SNLS3	WMAP7+DR7 +SNLS3+H_0
Flat, constant w:						
Ω_m	$0.262^{+0.023}_{-0.023}$	$0.329^{+0.034}_{-0.039}$	$0.246^{+0.020}_{-0.020}$	$0.267^{+0.017}_{-0.017}$	$0.284^{+0.019}_{-0.019}$	$0.269^{+0.015}_{-0.015}$
w	$-1.016^{+0.077}_{-0.079}$	$-0.826^{+0.166}_{-0.161}$	$-1.114^{+0.113}_{-0.113}$	$-1.110^{+0.122}_{-0.120}$	$-1.021^{+0.078}_{-0.079}$	$-1.061^{+0.069}_{-0.068}$
H_0	$71.58^{+2.41}_{-2.42}$	$64.42^{+4.25}_{-4.38}$	$74.11^{+2.58}_{-2.55}$	$72.21^{+2.46}_{-2.42}$	$69.77^{+2.07}_{-2.07}$	$71.57^{+1.65}_{-1.65}$
Non-flat, constant w:						
Ω_m	$0.259^{+0.050}_{-0.049}$	$0.312^{+0.051}_{-0.051}$	...	$0.253^{+0.021}_{-0.021}$	$0.294^{+0.021}_{-0.021}$	$0.271^{+0.015}_{-0.015}$
Ω_k	$0.001^{+0.015}_{-0.015}$	$-0.006^{+0.013}_{-0.012}$	...	$-0.012^{+0.008}_{-0.008}$	$-0.009^{+0.008}_{-0.008}$	$-0.002^{+0.006}_{-0.006}$
w	$-1.018^{+0.113}_{-0.110}$	$-1.027^{+0.379}_{-0.386}$	...	$-1.445^{+0.298}_{-0.292}$	$-1.068^{+0.094}_{-0.095}$	$-1.069^{+0.091}_{-0.092}$
H_0	$72.65^{+6.59}_{-6.73}$	$66.36^{+5.73}_{-5.87}$	...	$73.54^{+2.77}_{-2.79}$	$67.85^{+2.58}_{-2.57}$	$71.18^{+1.92}_{-1.87}$

[a]The values quoted are the expectation values of the marginalized distributions, not the best fits, with the 68.3% marginalized values quoted as the errors. All SN systematic uncertainties are included. Note that as the non-SN constraints used in CosmoMC differ slightly from those used in Table 2, the cosmological parameters are different. The closest comparison is SNLS3+WMAP7+DR7.

[b]We show only flat universe fits for the WMAP+H_0 combination; the fits were not constraining for non-flat cosmologies.

M.Sullivan et al. : SNLS3+

Class	Parameter	Const. w flat	Const. w non-flat
Primary	$100\Omega_b h^2$	$2.258^{+0.054}_{-0.054}$	$2.265^{+0.056}_{-0.056}$
	Ω_c	$0.1149^{+0.0041}_{-0.0041}$	$0.1145^{+0.0047}_{-0.0047}$
	θ	$1.0398^{+0.0026}_{-0.0027}$	$1.0401^{+0.0026}_{-0.0026}$
	τ	$0.087^{+0.006}_{-0.007}$	$0.088^{+0.007}_{-0.007}$
	Ω_k	$\cdots$	$-0.002^{+0.006}_{-0.006}$
	w_0	$-1.061^{+0.069}_{-0.068}$	$-1.069^{+0.091}_{-0.092}$
	n_s	$0.969^{+0.013}_{-0.013}$	$0.970^{+0.014}_{-0.013}$
	$\log[10^{10} A_{05}]$	$3.095^{+0.033}_{-0.033}$	$3.094^{+0.033}_{-0.033}$
	α	$1.451^{+0.109}_{-0.109}$	$1.454^{+0.112}_{-0.111}$
	β	$3.265^{+0.111}_{-0.111}$	$3.259^{+0.111}_{-0.109}$
Derived	Ω_{DE}	$0.731^{+0.015}_{-0.015}$	$0.731^{+0.015}_{-0.015}$
	Age[a]	$13.71^{+0.11}_{-0.11}$ Gyr	$13.78^{+0.31}_{-0.31}$ Gyr
	Ω_m	$0.269^{+0.015}_{-0.015}$	$0.271^{+0.015}_{-0.015}$
	σ_8	$0.850^{+0.038}_{-0.038}$	$0.847^{+0.038}_{-0.038}$
	z_{re}[b]	$10.55^{+1.20}_{-1.19}$	$10.55^{+1.20}_{-1.18}$
	H_0	$71.57^{+1.65}_{-1.65}$ km s^{-1} Mpc^{-1}	$71.18^{+1.92}_{-1.87}$ km s^{-1} Mpc^{-1}

M.Sullivan et al. : SNLS3+

- Flat + constant w + SNLS3 + SDSS BAO + WMAP7

$$\Omega_m = 0.276^{+0.019}_{-0.015},\ w = -1.043^{+0.080}_{-0.082}$$

  - Statistical errors: 5.2%
  - Systematic errors: 5.5%
    - Dominated by SN flux photometric calibration
    - Can be reduced to 2% without it

- Time variation of w: $w=w_0+w_a(1-a)$

$$\Omega_m = 0.271^{+0.015}_{-0.015},\ w_0 = -0.905^{+0.196}_{-0.196},\ w_a = -0.984^{+1.094}_{-1.097}$$

S.Meibom et al.: stellar rotation

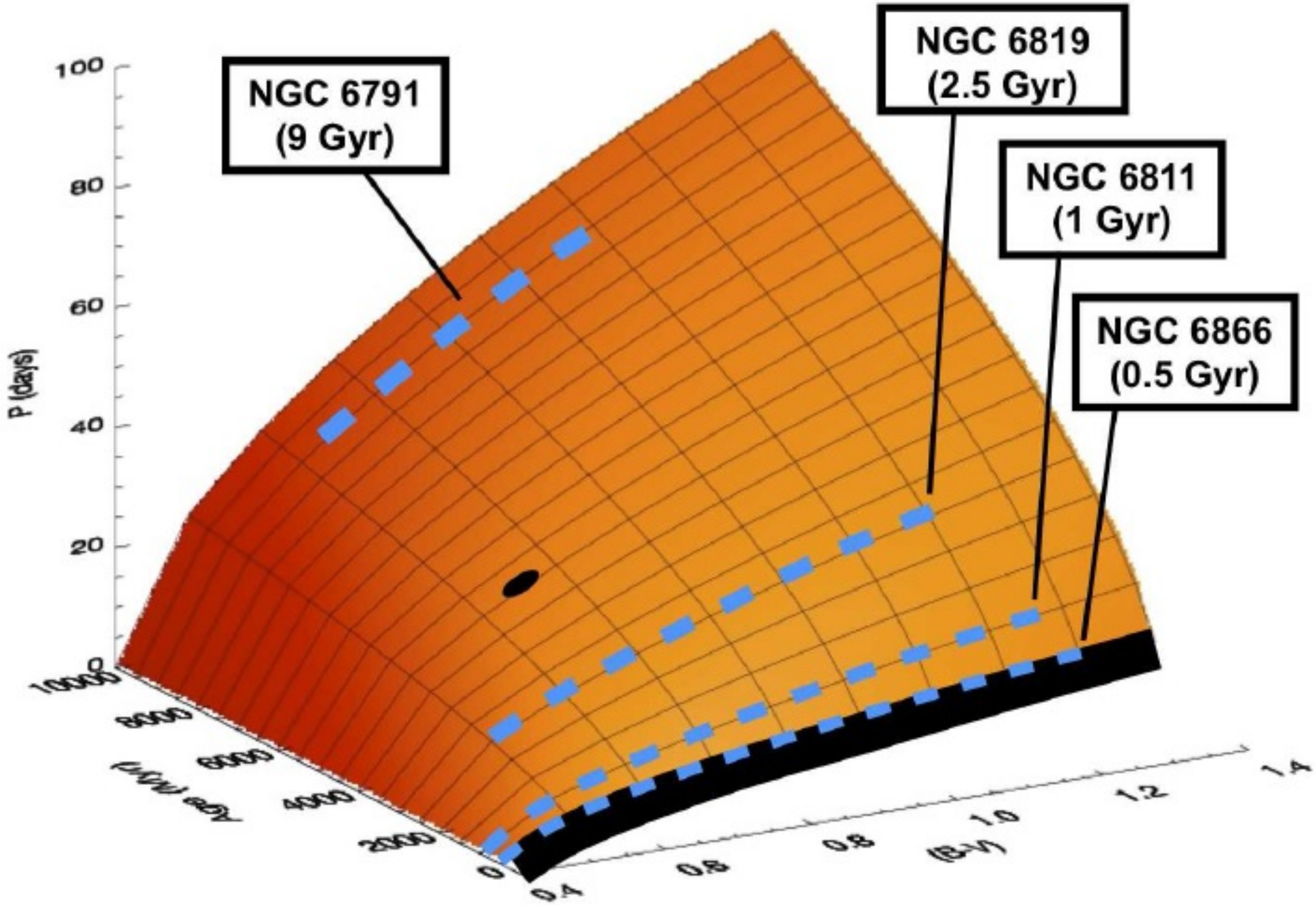

S.Meibom et al.: stellar rotation

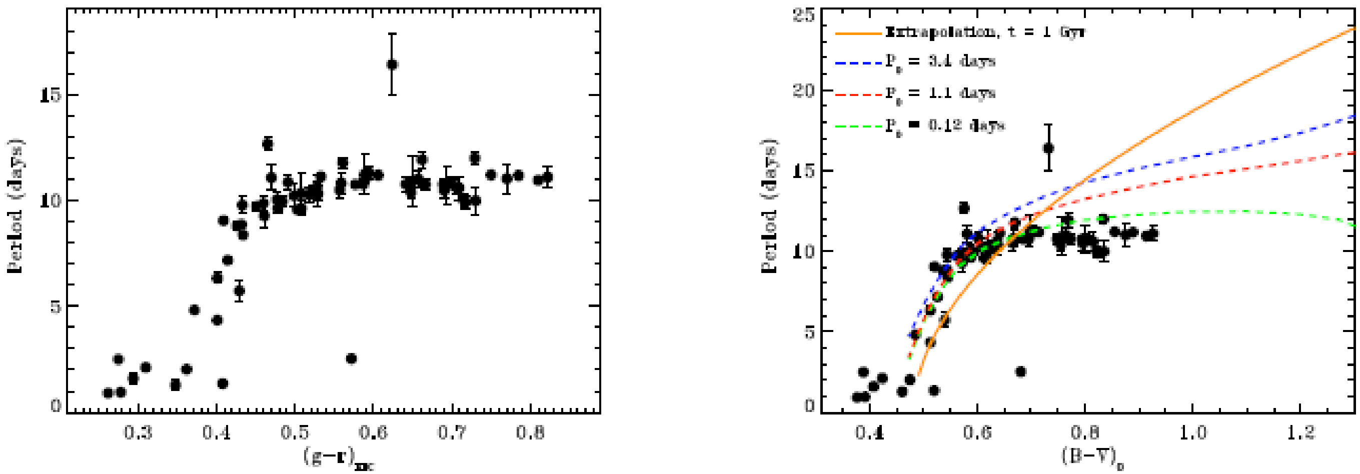

Fig. 4.— **Left:** The observed color-period diagram in *g-r* color for 71 FGK candidate single members of NGC 6811. The periods define a clear *I*-type sequence. The error-bars represent the RMS of multiple period measurements. The sequence is the observed representation of a cross-section at the age of NGC 6811 ($P = P(1\,\mathrm{Gyr}, M)$) of the surface $P = P(t, M)$. **Right:** The color-period diagram in de-reddened *B-V* color using $E_{(B-V)} = 0.1$. The orange curve represents the simple extrapolation to 1 Gyr, using the Skumanich $P \propto \sqrt{t}$ law, of the color-period relation from younger open clusters. The green, blue, and red curves are rotational isochrones for $t = 1\,\mathrm{Gyr}$ calculated using the rotational evolution theory described in Barnes (2010), and correspond to initial (ZAMS) periods of 0.12 days, 1.1 days, and 3.4 days respectively.

Schlighting & Chang: planetary rings

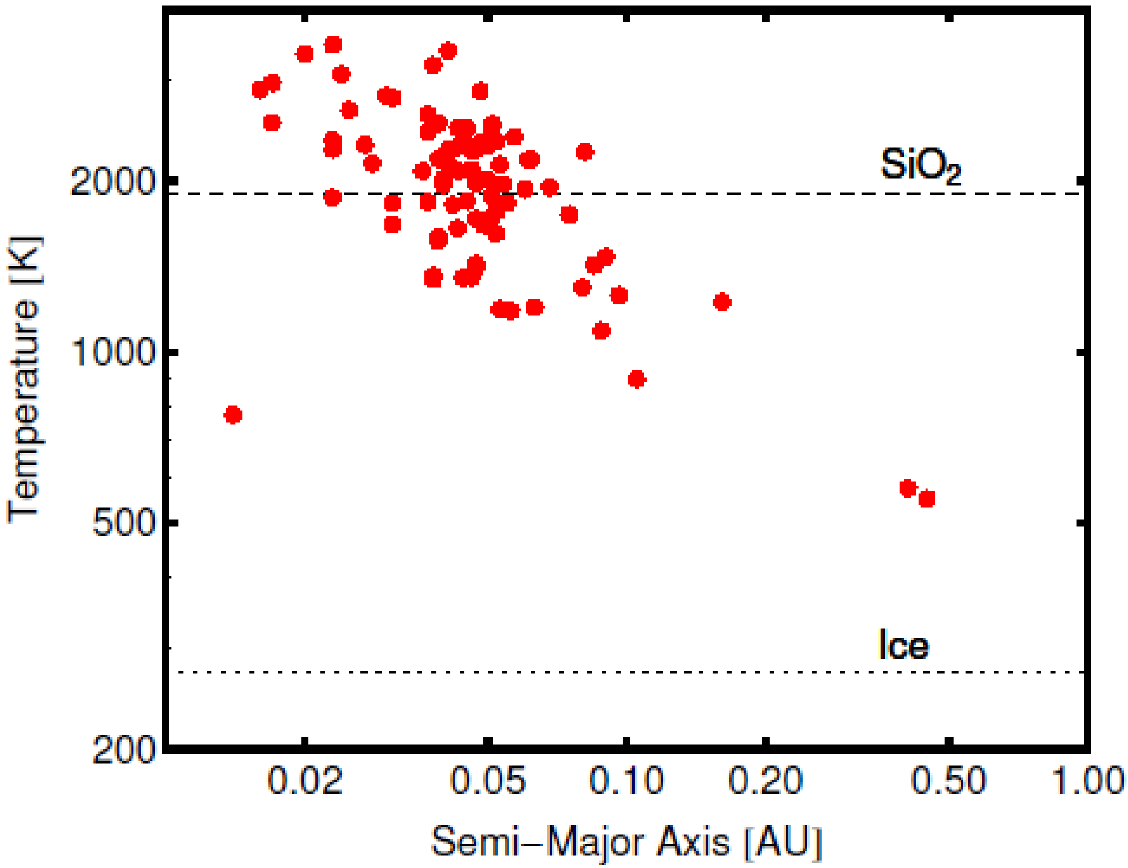

Figure 1. Equilibrium blackbody temperature for ring particles for known transiting extrasolar planets. The melting temperature of water ice (dotted line) and silicon dioxide (SiO_2) (dashed line) are plotted for comparison. Exoplanet data is taken from Wright et al. (2010) (http://exoplanets.org).

Schlighting & Chang: planetary rings

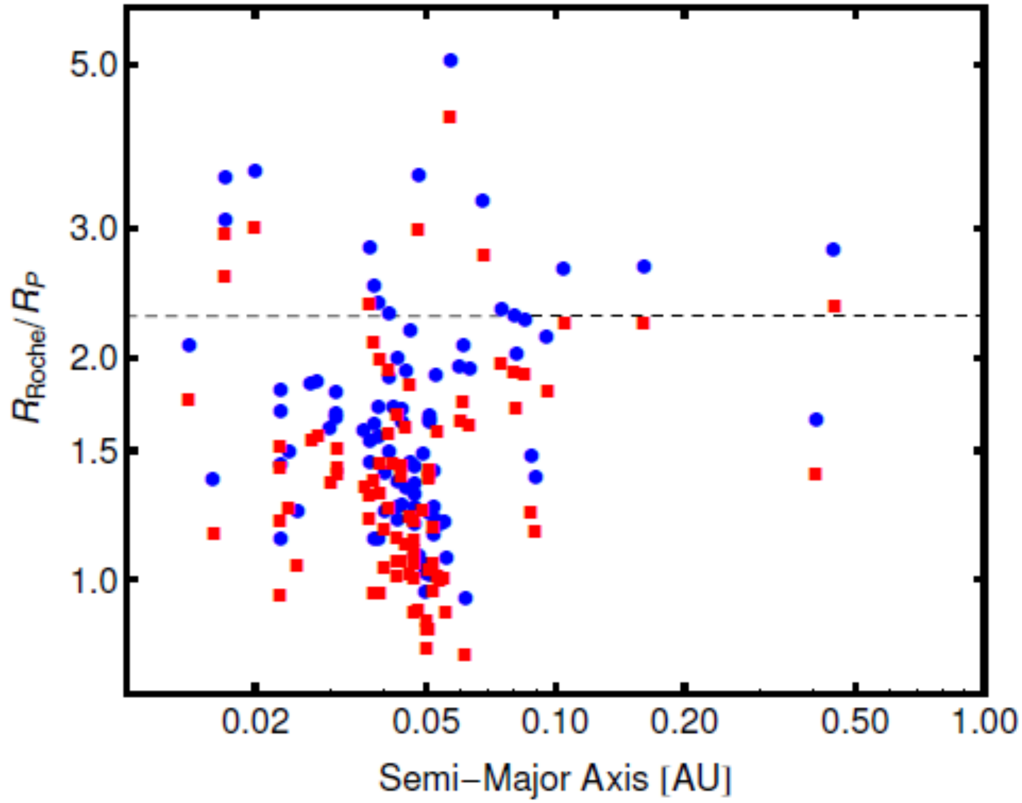

Figure 2. Roche radius, $R_{\rm Roche}$, of currently known transiting extrasolar planets for a particle density of 3 (blue circles) and $5\,{\rm g\,cm^{-3}}$ (red squares). The dashed line corresponds to Saturn's Roche radius with a mean density of $\rho_{\rm P} = 0.7\,{\rm g\,cm^{-3}}$ and for icy ring particles with a density of $\rho = 1\,{\rm g\,cm^{-3}}$. It is clear from this plot that a significant number of extrasolar planets have Roche radii that allow for the existence of rings. The exoplanet data are taken from Wright et al. (2010) (http://exoplanets.org).

Schlighting & Chang: planetary rings

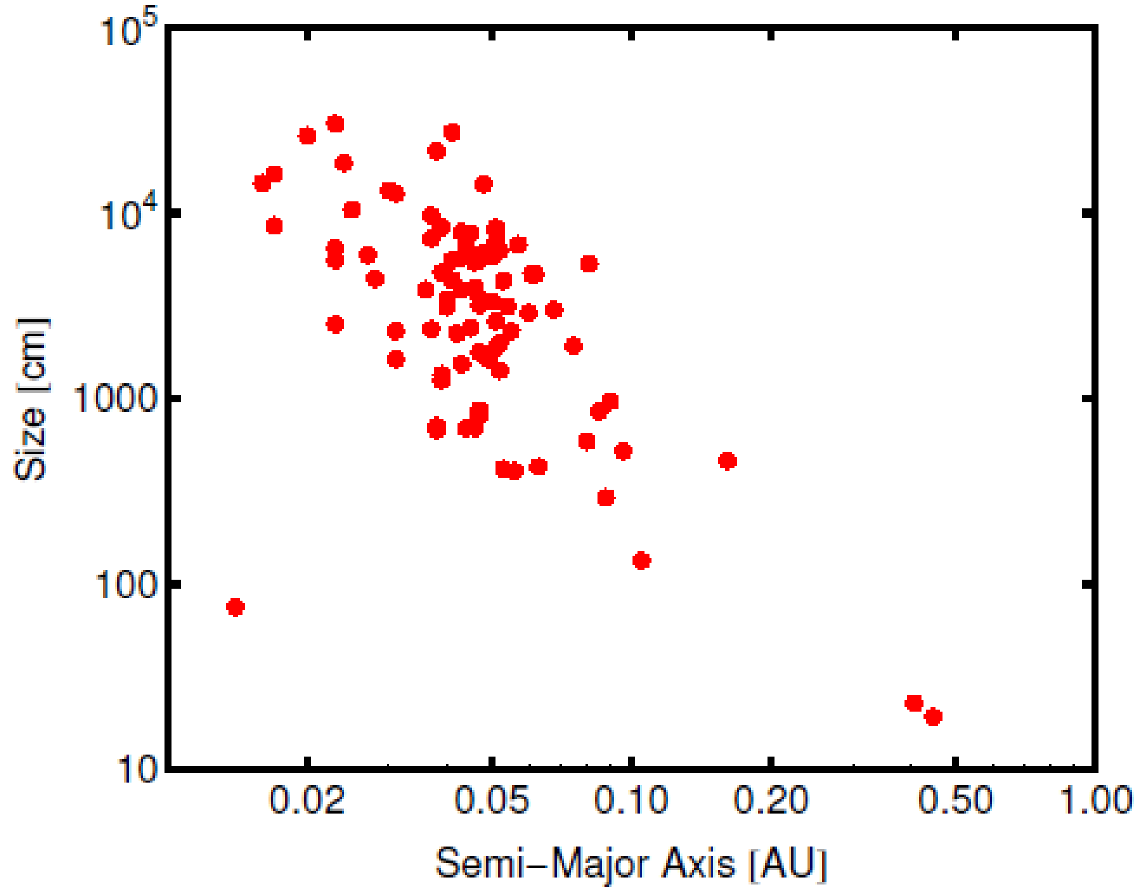

Figure 3. The smallest ring particle size for which $t_{\rm PR} > 10^8$ years of known transiting extrasolar planets. The Poynting-Robertson timescale, $t_{\rm PR}$, was evaluated assuming $Q_{\rm PR} \sim 0.5$ and $i \sim 45°$. The exoplanet data used in this calculation are from Wright et al. (2010) (http://exoplanets.org).

Schlighting & Chang: planetary rings

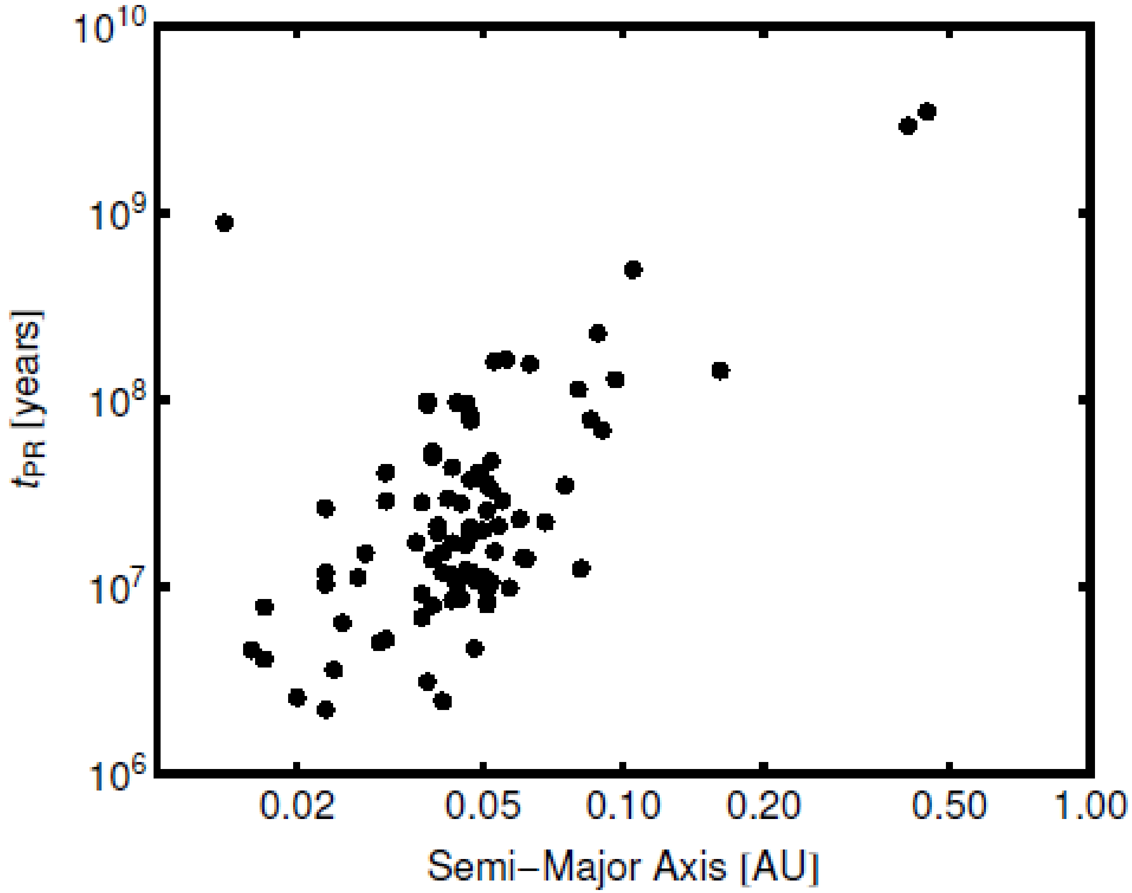

Figure 4. Ring lifetimes due to Poynting-Robertson drag assuming optically thick planetary rings around known transiting extrasolar planets. The Poynting-Robertson timescale, $t_{\rm PR}$, was evaluated assuming $Q_{\rm PR} \sim 0.5$, $i \sim 45^\circ$ and $\Sigma \sim 400$ g cm^{-2}.

Schlighting & Chang: planetary rings

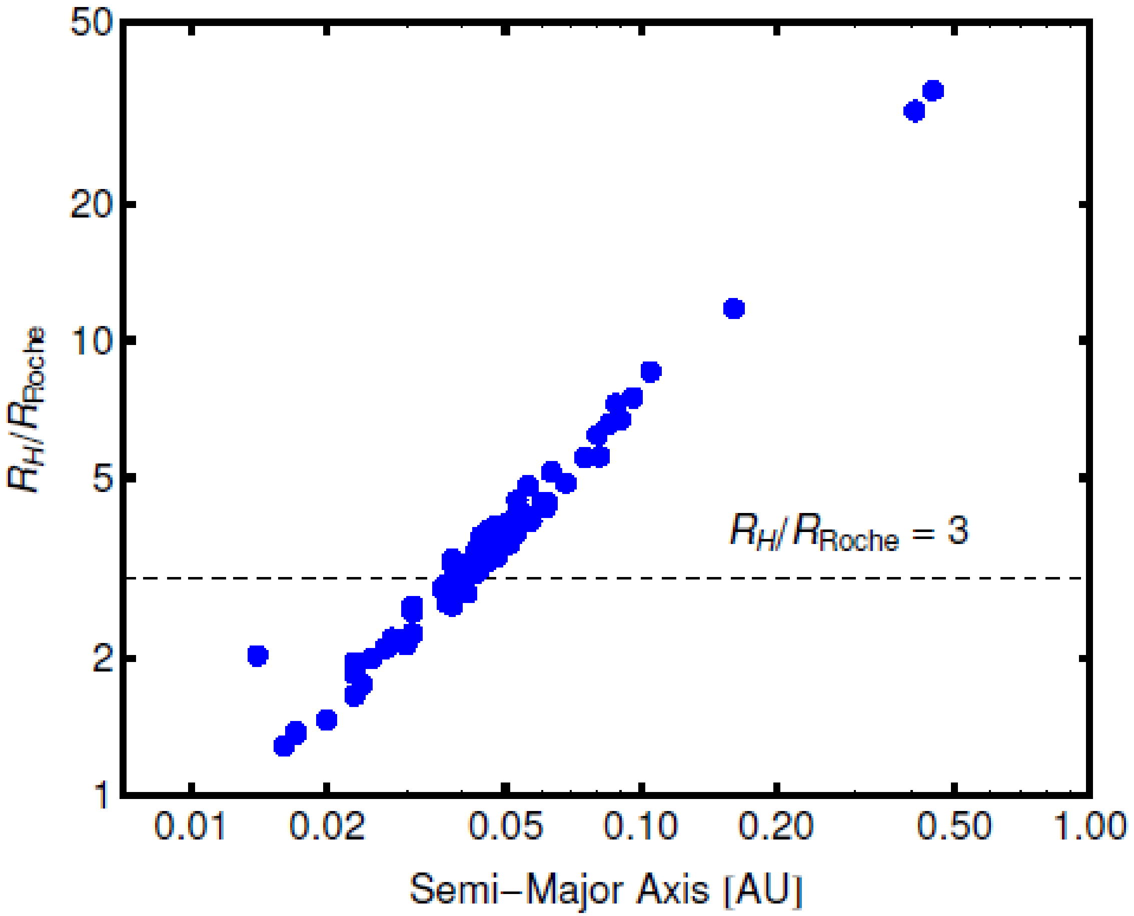

Figure 5. Ratio of the Hill radius, R_H, to the Roche radius, R_{Roche}, of known extrasolar planets. The dashed line corresponds to $R_H/R_{Roche} = 3$. The exoplanet data are taken from Wright et al. (2010) (http://exoplanets.org)

Schlighting & Chang: planetary rings

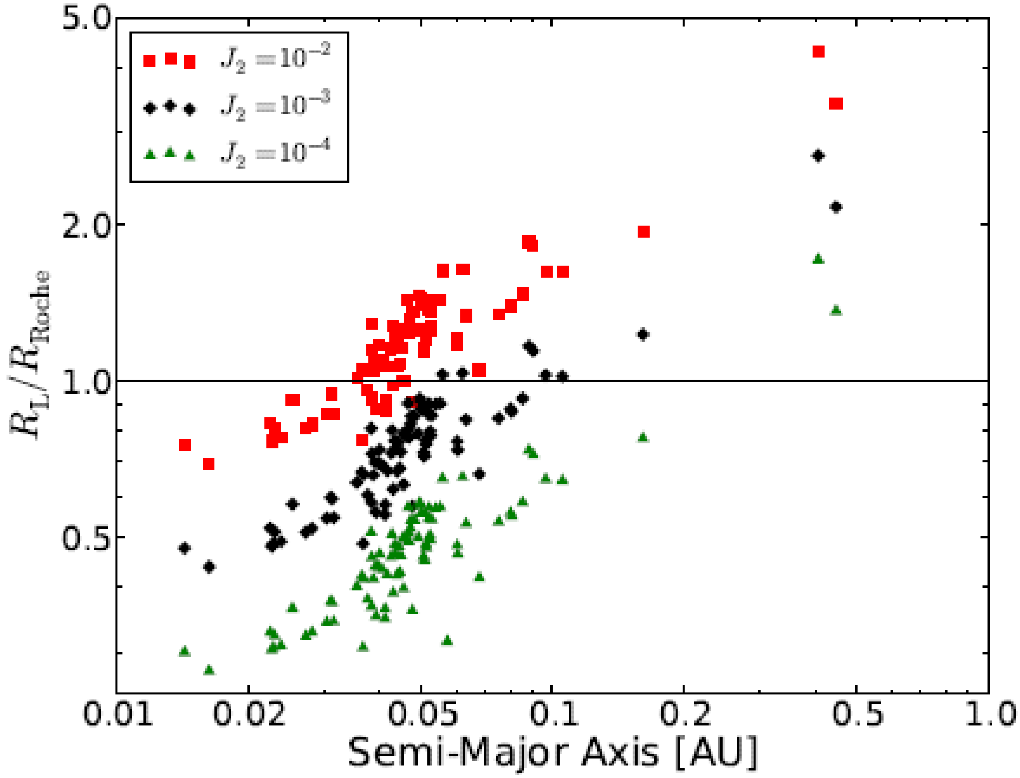

Figure 6. Ratio of the Laplace radius to the Roche radius for ring material with a density of $3\,\mathrm{g\,cm^{-3}}$ and $J_2 = 10^{-4} - 10^{-2}$. The solid line marks where $R_L = R_{Roche}$. Above this line, the rings will mostly lie in the plane defined by the planet's equator. Whereas below this line, the rings will undergo a transition from lying in the planet's equatorial plane at small r to lying in the orbital plane at large r. The exoplanet data used in this calculation are from Wright et al. (2010) (http://exoplanets.org).